

Serum Glycomics Profiling of Patients with Primary Restless Legs Syndrome Using LC–MS/MS

Xue Dong,¹ Stefania Mondello,¹ Firas Kobeissy, Raffaele Ferri, and Yehia Mechref*Cite This: *J. Proteome Res.* 2020, 19, 2933–2941

Read Online

ACCESS |

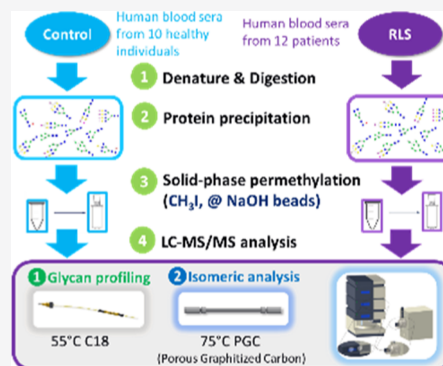
Metrics & More

Article Recommendations

Supporting Information

ABSTRACT: Restless legs syndrome (RLS), also known as Willis–Ekbom disease, is a sleep and neurological sensorimotor disorder. The prevalence of RLS is at ~5–15% in the general population. RLS could severely impact the daytime work productivity and the life quality of patients. However, the current diagnostic methods fail to provide an accurate and timely diagnosis, and the pathophysiology of RLS is not fully understood. Glycomics can help to unravel the underlying biochemical mechanisms of RLS, to identify specific glycome changes, and to develop powerful biomarkers for early detection and guiding interventions. Herein, we undertook a shotgun glycomics approach to determine and characterize the potential glycan biomarker candidates in the blood serum of RLS patients. Glycan profiles and isomeric quantitations were assessed by liquid chromatography–mass spectrometry analysis and compared with healthy controls. 24 *N*-glycan biomarker candidates show substantial differences between RLS patients and controls after the Benjamini–Hochberg multiple testing correction. Among those structures, glycans with the composition of HexNAc₆Hex₃Fuc₁NeuAc₂, HexNAc₆Hex₆Fuc₁NeuAc₃, and HexNAc₃Hex₆Fuc₁NeuAc₂ show the most significant alteration in the expression profile ($p < 0.001$). Furthermore, 23 isomeric structures in the RLS cohorts show significant differences after the Benjamini–Hochberg multiple testing correction. HexNAc₄Hex₅Fuc₁NeuAc₂ (4512-3) and HexNAc₆Hex₇NeuAc₃ (6703-1) ($p < 0.001$) were downexpressed in the RLS cohort. HexNAc₆Hex₇NeuAc₃ (6703-2) and HexNAc₃Hex₆NeuAc₃ (5603-5) ($p < 0.001$) were expressed higher in the RLS cases. These results demonstrate that it is possible to detect specific glycome traits in individuals with RLS. The discovery of the *N*-glycan expression alterations might be useful in understanding the molecular mechanism of RLS, developing more refined and objective diagnostic methods, and discovering novel targeted therapeutic interventions.

KEYWORDS: idiopathic RLS, *N*-glycans, isomers, biomarker, neurological disorder, LC–MS/MS



INTRODUCTION

Restless legs syndrome (RLS), also known as Willis–Ekbom disease, is a sleep and neurological sensorimotor disorder,^{1–3} with a prevalence of ~5–15% in the general population.^{2,4,5} The patients who suffer from RLS experience an irresistible or involuntary movement of their legs. The symptoms are even worse in static conditions such as during sleep or in confined spaces such as sitting in a plane while traveling. Besides disrupting sleeping, RLS also severely impairs a patient's daytime work productivity and quality of life. Recent studies have shown that RLS is related to cardiovascular disease.^{4–6}

To date, the diagnosis of RLS has been based on international consensus criteria,⁷ which predominately rely on clinical signs and patient-reported symptoms.^{1,5,8} Those empirical criteria are not informative enough to support an accurate and timely diagnosis. Therefore, there is an urgent need to develop molecular biomarkers to support the diagnosis, prognosis, and to guide disease management and treatment. The application of neuroproteomics has been found to be a novel and powerful strategy of identifying biomarker candidates in neurological and sleep disorders with unpre-

cedented accuracy and sensitivity.^{9,10} The results from different groups showed substantial alterations in several proteins between RLS patients and controls.^{4,5} Nonetheless, the quest is still ongoing and new approaches are needed to advance our knowledge of the pathogenetic and pathophysiological mechanisms involved in RLS.

Recent advances and applications of high-resolution mass spectrometry (MS) have permitted the analysis of post-translational modifications such as glycosylation, acetylation, or phosphorylation. Glycosylation, in particular, has an impact on the biological and pathobiological functions of proteins^{11–15} because protein properties, such as stability and activity, can be deeply influenced by glycosylation.¹⁶ Altered glycomics profiles and aberrant expressions in glycans have been reported in

Received: August 13, 2019

Published: June 2, 2020



association with neurological disorders, and have been suggested as novel diagnostic and prognostic tools.^{11,17} However, to our knowledge, no studies have been conducted to investigate the glycosylation or glycome changes associated with RLS. Such work would provide novel insight and a better understanding of the molecular mechanisms of RLS. In addition, the identification of biomarker candidates could permit and support the development of novel RLS diagnostic methods and therapeutic treatments.

With these aims in mind, we analyzed and characterized glycan profiles and quantified glycome alterations in the blood of RLS patients by using reversed-phase liquid chromatography (LC)–MS on permethylated glycans. Such an analytical methodology increases efficiency,¹⁸ separation resolution, and sensitivity.^{17,19,20} Furthermore, we performed an in-depth glycomic analysis of the isomeric structures given that different glycan isomers can have completely different biological functions. The isomers were identified and quantified using porous graphitized carbon (PGC) LC–MS.

■ EXPERIMENTAL SECTION

Study Participants

The study protocol was approved by the local ethics committee. Patients were enrolled at the Sleep Research Centre of the Oasi Research Institute—IRCCS, Troina (Italy), and at the Department of Neurology of the University of Bologna (Italy), between March 2017 and August 2017. The patients with primary RLS were clinically diagnosed according to the internationally standardized criteria (International RLS Study Group criteria⁷). In addition to the diagnosis of RLS, enrollment in the study depended on the following inclusion criteria: (1) patient age \geq 18 years, (2) drug naïve, (3) availability of at least one blood sample for analysis, and (4) signed consent. Patients with other neurological or medical conditions or if they were pregnant or taking any medications were excluded. As a comparison group, age-matched healthy individuals were also enrolled. Criteria for control subject enrollment included age \geq 18 years and no history of brain injury, neurological, or psychiatric disorder. All participants provided written informed consent.

Blood Sampling

Blood samples were collected between 9 a.m. and noon by venipuncture into gel separator tubes for serum. Blood tubes were rapidly transported to the laboratory facility of the hospitals and centrifuged within 1 h after blood collection. Serum was immediately aliquoted into cryovials and stored at -80 °C until it was shipped on dry ice to the Core Lab (Lubbock, TX) for analysis. The analysts were blinded to participants' diagnosis and clinical status.

Materials and Reagents

PNGase F and G7 buffer (50 mM sodium phosphate buffer, pH 7.5) were from New England Biolabs (Ipswich, MA, USA). Ammonium–borane complex, CH₃I iodomethane, dimethyl sulfoxide (DMSO), and NaOH beads were purchased from Sigma-Aldrich (St. Louis, MO, USA), ethanol was from PHARMCO-AAPER, and HPLC grade methanol, acetonitrile (ACN), formic acid, and HPLC water were obtained from Fisher Scientific (Fair Lawn, New Jersey, USA).

Sample Preparation

The preparation and analysis order of control and RLS samples were disrupted to avoid biases introduced by batch effects. N-

Glycans were released and purified from the glycoproteins in the blood sera according to previous protocols.^{11,21} Briefly, an aliquot of 10 μ L serum was taken from each participant blood sample. Ten times diluted sodium phosphate buffer was added into each sample vial and denatured for 20 min at 90 °C. Then, N-glycans were released by PNGase F digestion for 18 h at 37 °C. An ice-cold ethanol solution (90% ethanol v/v) was added into the mixture after enzymatic digestion. The supernatant containing purified N-glycans was collected and dried in a spin vacuum drier. After that, glycans were reduced with an ammonium–borane complex at 60 °C for 1 h. The excess reducing reagent was washed off with 500 μ L methanol 4–5 times and dried in a spin vacuum.

The reduced N-glycans were permethylated with a solid-phase permethylation protocol, as previously described.^{21–23} The dried N-glycans were reconstituted in a solution containing 30 μ L DMSO, 20 μ L iodomethane, and a trace amount of water (ca. 1.2 μ L). Sodium hydroxide beads stored in DMSO were packed in spin columns with a pipette, rinsed with around 100 μ L DMSO, and spun down by low-speed centrifugation. The sample solution was then loaded into the packed spin column and incubated for 25 min at room temperature. An additional 20 μ L iodomethane was added into the spin column, incubated for another 15 min, and centrifuged at 1.8k rpm. The collected solutions were dried overnight in a spin vacuum drier. Permethylated N-glycans derived from blood sera were resuspended in 20% ACN containing 0.1% formic acid before injection in LC–MS.

LC–MS Conditions

All samples of the control and the RLS cohorts were analyzed under both C18 and PGC-LC–MS conditions for glycan profiles and isomeric quantitative analysis using an UltiMate 3000 nano-LC system (Dionex, Sunnyvale, CA, USA) coupled with an LTQ Orbitrap Velos mass spectrometer (Thermo Scientific, San Jose, CA, USA). The same mobile phase compositions were used under C18 and PGC separation conditions. The mobile phase A was 98% HPLC water, 2% ACN containing 0.1% formic acid; mobile phase B consisted of 100% ACN and 0.1% formic acid. After LC separation, analytes were detected in the mass spectrometer in positive mode. The resolving power of the instrument was set to 100,000. The full MS spectra were obtained in the mass range of 700–2000 m/z with a mass accuracy of 5 ppm.

Glycan Profiling Conditions

Glycan profiles were obtained on a reversed phase Acclaim PepMap capillary column (150 mm \times 75 μ m i.d.) packed with the 100 Å C₁₈-bonded phase (Dionex) at 55 °C under optimized LC conditions.^{21,24,25} The flow rate was 0.35 μ L/min. The eluting gradient started with 20% mobile phase B over 10 min, ramped to 42% of mobile phase B in 1 min, then gradually increased to 55% B over 37 min, ramped to 90% B in 1 min and kept there for 5 min, decreased to 20% B in 1 min, and maintained for 5 min.

Isomeric Profiling Conditions

Isomeric analysis was performed on a HyperCarb PGC column (75 μ m \times 100 mm, 5 μ m particle size; Thermo Scientific, Pittsburgh, PA) at 75 °C. The PGC separation conditions used in this study refer to the optimized conditions as we previously reported.^{26,27} The flow rate was 0.75 μ L/min. The elution gradient began with 20% of mobile phase B for 10 min, 20–

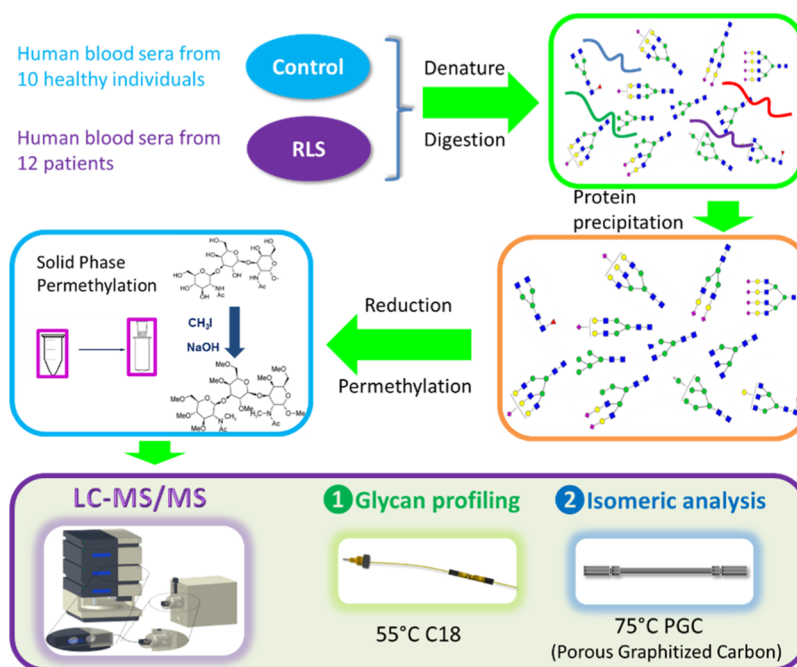


Figure 1. A flowchart summarizing sample preparation and analysis.

60% B (10–30 min), 60–95% B (30–40 min), and 95% B was maintained for 20 min.

Data Processing and Quantitation by MultiGlycan-ESI Quantification

Quantitative glycan profiling results were obtained using MultiGlycan software with datasets acquired from C18-LC-MS. The algorithms and quantitation reliability were assessed in previous works.^{28,29} Briefly, glycan compositions were identified by searching for the experimental m/z values of monoisotopic peaks of ions in the MS spectra against the default database built into the software. Mass accuracy of 5 ppm was employed, isotopic envelope tolerance was set to 6 ppm. All possible charge states and adducts of a glycan composition were considered. The output quantitation results were reported as the sum of matched charge states and adducts ($[M + H]^+$, $[M + 2H]^{2+}$, $[M + 3H]^{3+}$, $[M + NH_4]^+$, and $[M + 2NH_4]^{2+}$) of a certain glycan composition.

Isomeric structures were identified and quantified with datasets acquired on PGC-LC-MS. First, glycan compositions were identified by searching the experimental m/z values of the monoisotopic peaks in the MS spectra against theoretical m/z values in the default database. Then isomeric structures were assigned by the eluting order of the isomeric peaks based on the glycan isomer database from previous works.^{26,27} Quantification of isomers was obtained by calculating the peak area of glycan ions of all charge states and adduct ions using Xcalibur. The glycan quantitative results were normalized and reported as relative abundances, which were calculated by using the peak area of each glycan structure versus the total structures identified in each sample.

Statistical Analysis

Initial analyses examining the differences in characteristics between subjects with RLS and controls were assessed by using a t -test (for age—normally distributed continuous variable) and a Fisher's exact test (for smoking status—categorical variable).

N -Glycan structures and isomers that were significantly altered were identified by performing a nonparametric Mann–Whitney U test. After the statistical tests, the Benjamini–Hochberg procedure was applied for the multiple testing correction at a 0.05 false discovery rate to control the type-I error.

The group properties of the 12 blood serum samples of participants with RLS and 10 healthy control samples were analyzed by principal component analysis (PCA). Unsupervised PCA without designation was performed on datasets acquired on C18-LC-MS and PGC-LC-MS with MarkerView software, the settings of parameters were referred to one of our previous biomarker discovery studies.³⁰ The results in our previous studies analyzing biological samples have proved the reproducibility and reliability of the sample preparation and instrumental analysis methods, and have demonstrated that the replicates would not affect the data point distributions in the PCA plots.^{31,32}

RESULTS AND DISCUSSION

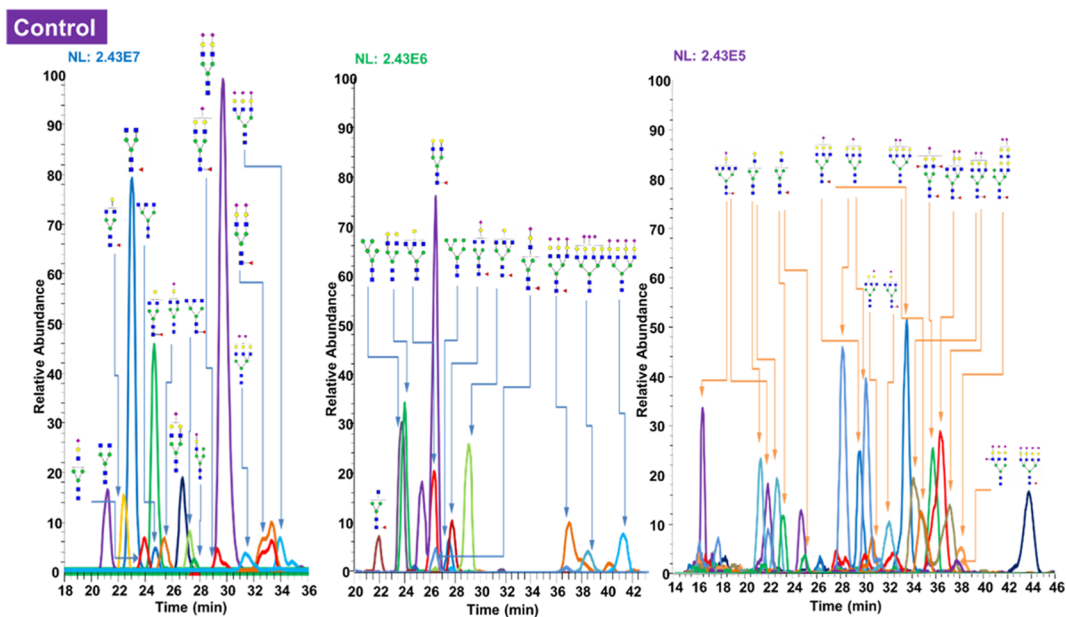
Description of Study Population

Serum samples were collected from 12 patients with a clinical diagnosis of primary RLS (8 females and 4 males and a mean age of 68.52 years [$SD \pm 8.01$]) and 10 healthy controls (5 females and 5 males and a mean age of 67.61 years [$SD \pm 15.07$]). No significant difference in age and cigarette smoking habits were found between the patients and controls ($p > 0.05$).

N -Glycan Profile of the Control and Idiopathic RLS Cohorts

The N -glycan profiles of the control and RLS cohorts were acquired by the analysis of reduced and permethylated glycans on C18-LC-MS, as shown in the flowchart (Figure 1). Figure 2 shows the illustrative examples of extracted ion chromatograms (EICs) of a control subject and a patient with RLS. The retention times, relative intensities, and structural features of the identified glycan structures are presented in the EICs.

(a)



(b)

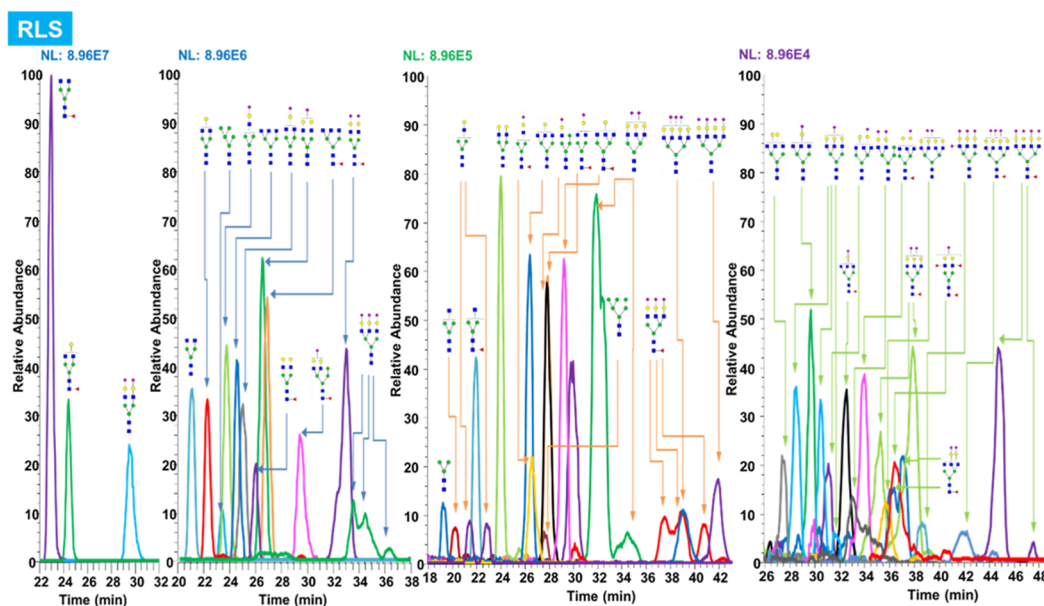


Figure 2. EIC of permethylated glycans derived from the blood samples of (a) control and (b) patient with RLS. The identified glycans are displayed in separate panels based on their intensity magnitude to make sure all structures are visible. Symbols: blue \square , *N*-acetylglucosamine (GlcNAc); yellow \circ , Galactose (Gal); red ∇ , Fucose (Fuc); green \circ , Mannose (Man); blue \circ , Glucose (Glc); and magenta \diamond , *N*-acetylneuraminic acid (NeuAc/sialic acid).

Glycan profiling data for all samples of control and RLS cohorts are listed in Tables S1 and S2. In total, 60 *N*-glycans in the control cohort and 57 *N*-glycans in the RLS cohort were identified and quantified.

When relative intensities of the glycans were averaged per cohort, the top three abundant glycan structures in controls were disialylated glycans with the composition of HexNAc₄Hex₅NeuAc₂, monosialylated glycan HexNAc₄Hex₅NeuAc₁, and monofucosylated glycan with the composition of HexNAc₄Hex₃Fuc₁ (43, 18, and 7% average abundance,

respectively), as shown in Table S1. In terms of the abundance of different types of glycans shown in Table S1, we observed that 38 out of the total 60 glycans contain sialic acid, which account for 77% in the control cohort. Nine structures were fucosylated glycans, which represent 14% of the total. Thirteen structures were high-mannose type, which account for 9% of the total glycan profile. In comparison, in the RLS cohort, the most abundant structures on average were HexNAc₄Hex₅NeuAc₂, HexNAc₄Hex₅Fuc₁NeuAc₁, and HexNAc₄Hex₃Fuc₁ (relative abundances 16, 12, and 12%, respec-

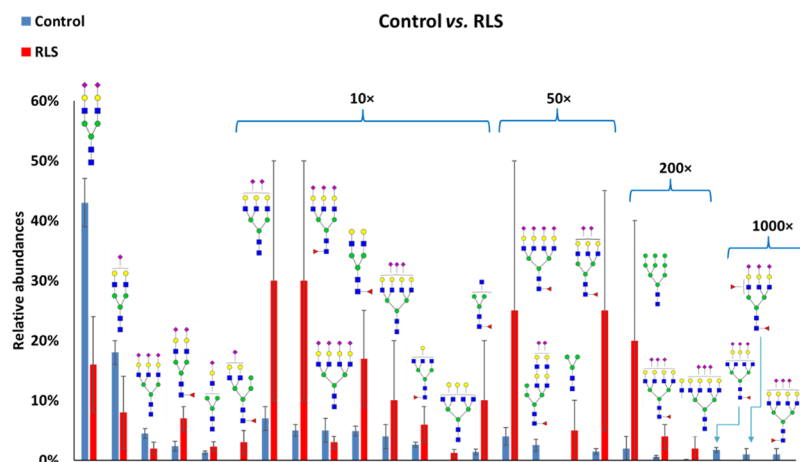


Figure 3. Bar graphs of the LC–MS relative abundances of permethylated *N*-glycan with significant differences between control and RLS cohorts after the Benjamini–Hochberg multiple testing correction was performed. (10 \times , 50 \times , 200 \times , and 1000 \times in the figure represent abundances magnified 10 times, 50 times, 200 times, and 1000 times, respectively.) Symbols: see Figure 2.

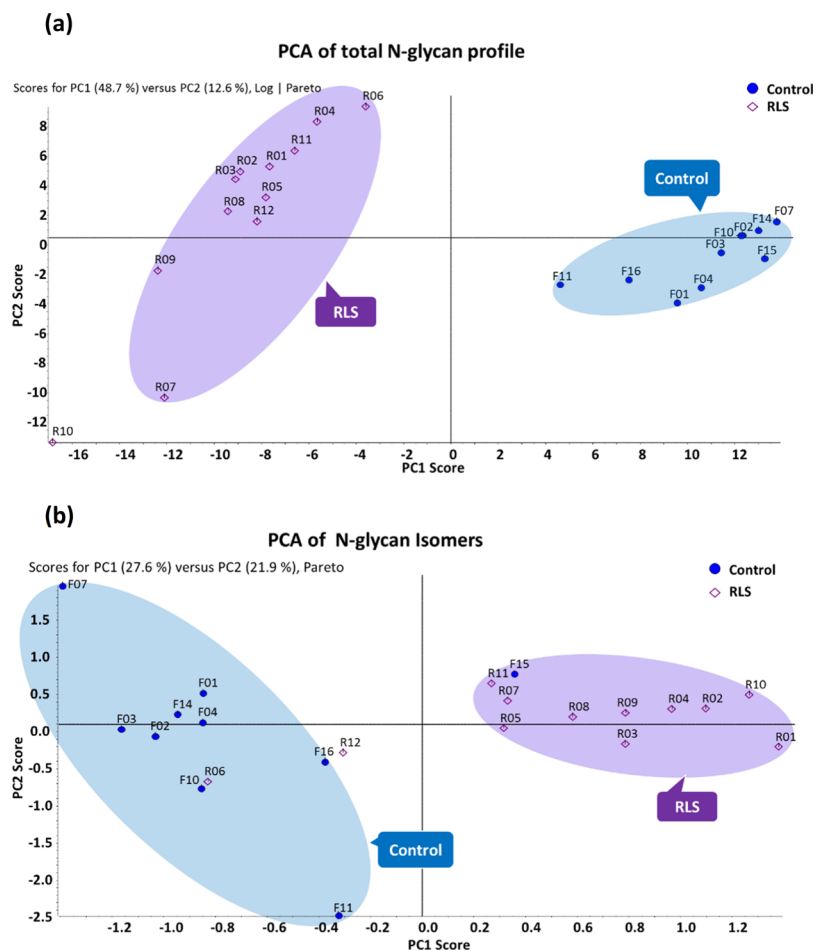


Figure 4. (a) The PCA plot of the total *N*-glycan profile. (b) The PCA plot of *N*-glycan isomers.

tively), as shown in Table S2. In terms of the distribution of different types of glycans shown in Table S2, 33 sialylated glycans, 10 fucosylated glycans, and 14 high mannose glycans were discovered. According to relative abundances in the RLS cohort, sialylated glycans stand for 67% of all glycans, fucosylated structures account for 22%, and high-mannose type is 13%.

Statistical Analysis of the Control and Idiopathic RLS Cohorts

The differently expressed glycan structures between the control and the RLS cohorts are shown as bar graphs in Figure 3 and the corresponding *p*-values from the Mann–Whitney *U* tests are listed in Table S3. Based on the statistical test results, 24 *N*-glycan structures showed a significant difference between the control and the RLS cohorts after applying the Benjamini–

Hochberg corrections. Those glycans can be the candidates for discovery of potential glycan biomarkers to distinguish RLS from healthy individuals. Among them, 18 structures are sialylated glycans, 13 structures are fucosylated, and 2 structures are high-mannose type, suggesting that sialylated glycans may play an important role in RLS. Our previous glycomics studies on other diseases also reported that sialylated glycans are differently expressed in diseased groups and deserve further investigation as potential biomarker candidates.^{11,14} Furthermore, 23 structures show the most substantial difference in expression, with *p*-values of less than 0.001 (Table S3). Glycans with the composition of HexNAc₆Hex₃Fuc₁NeuAc₂, HexNAc₆Hex₆Fuc₁NeuAc₃, and HexNAc₅Hex₆Fuc₁NeuAc₂ are the structures with the lowest *p*-values. However, those structures are very low in abundance, which may cause difficulties in applications for clinical use. In the glycan candidate list (Table S3), HexNAc₄Hex₅NeuAc₂ and HexNAc₄Hex₅NeuAc₁ are more abundant in both the RLS and the control blood sera. They may be better candidates for further biomarker verification analysis.

PCA was performed to see if the control cohort and the RLS cohort have different serum glycan profiles that can separate the two cohorts. Relative abundances of glycans of all samples from the control and the RLS cohorts in Tables S1 and S2 were used to plot PCA (Figure 4a). We observed that the sample points of the control and the RLS cohorts clearly clustered into two distinct groups and were located in different regions of the PCA plot, which indicates that the different glycan structure distributions in the glycan profiles could reflect biological and pathological characteristics of the control and the RLS cohorts, respectively.

The *N*-glycan structural features found in RLS were compared with those reported in the study of rapid eye movement sleep behavior disorder (RBD), which is a parasomnia that is regarded as one of the earliest signs of neurodegenerative disorders (Table 1).¹¹ Both RLS and RBD studies show significant glycan changes in structural complexity and most of those are sialylated structures. In terms of structural complexity, the biomarker candidates in RLS tend to have more tetra-antennary and less diantennary glycans than RBD. In addition, glycans in RLS have a higher degree of sialylation (less mono sialylation, more with di-, tri-, and tetrasialylation) at the terminus than those in RBD. However, the increase in glycan structural complexity and a higher level of tri- and tetra-sialylation in blood sera of diseased cases were also discovered in cancer studies (e.g. breast or liver cancer).¹⁷

Also, we compared the potential *N*-glycan biomarker candidates with a glycomics study of leukodystrophy (related to eIF2B mutations), which is a brain development disorder that causes abnormal development or destruction of the white matter in the brain (Table 1).³³ The study was based on comparative analysis of cerebrospinal fluid (CSF) from healthy and diseased cases. Increased diantennary structures and decreased triantennary structures in the *N*-glycan profiles were observed. 11 glycan structures were found to have significant changes in the diseased cohort versus the control cases. Only 18% of those potential biomarkers contained sialic acid (mono or disialic acids at the terminus).

In future studies, animal experiments and clinical research are necessary to understand the biofunctions of these differentially expressed glycan structures, which could be potential biomarker candidates as well as therapeutic targets.

Table 1. *N*-Glycan Structures Expressed with Significant Differences after Correction for Multiple Comparison in RLS Cases Were Compared with Significant Glycan Changes Identified in RBD¹¹ and Leukodystrophy (Related to eIF2B Mutations)^{33a}

diseases and types	sample sources	RLS neurological disorder		RBD parasomnia (an early sign of neurodegenerative disorders)		leukodystrophy (eIF2B mutations) brain developmental disorder	
		blood serum	blood serum	blood serum	CSF	CSF	CSF
complexity comparison	diantennary	4	17%	6	38%	5	45%
	triantennary	6	25%	5	31%	6	55%
	≥tetraantennary	8	33%	2	31%	0	0%
number of sialic acids	mono	3	13%	5	31%	1	9%
	di	5	21%	2	13%	1	9%
	tri	8	33%	0	0%	0	0%
	≥tetra	2	8%	1	6%	0	0%
number of structures in common (vs RLS)	2 (4510, 6600)				2 (4510, 4502)		

^aThe number of structures under different comparing conditions and their percentages relative to the total number of significantly different structures discovered in the corresponding disease studies are listed.

Isomeric Quantitative Analysis of the Control and Idiopathic RLS Cohorts

Isomeric structure identification and quantitation has become an unneglectable part of in-depth glycomics analysis given different functions of isomers in biological processes. Thus, in this study, after glycan profiling, we analyzed the glycan samples of both the control and the RLS cohorts on the PGC column at 75 °C for isomeric analysis. Glycans with significant differences in the glycan profiles were investigated in isomeric structure identification and quantitation. In total, 38 isomeric structures for 13 glycan compositions for both cohorts were identified and quantified as the ratio of different isomers present in the samples. Eleven of those glycan compositions contain at least one sialic acid moiety. Detailed quantitation results of the control cohort and the RLS cohort are given in Tables S4 and S5, respectively.

Statistical Analysis of Isomers in the Control and Idiopathic RLS Cohorts

The ratios of the isomeric structures (Tables S4 and S5) were used to perform a nonparametric Mann–Whitney *U* test. Isomeric structures with significant differences in the control and RLS cohorts, after Benjamini–Hochberg corrections, are shown as bar graphs in Figure S1. The specific quantitation results are summarized in Table S6 (the isomeric structures that cannot be confidently assigned are differentiated by their elution order). Fifteen of those isomeric structures showed a significant difference between the control and RLS cohorts after performing corrections for multiple testing. The glycans showing the most significant differences (*p* < 0.001) were HexNAc₄Hex₅Fuc₁NeuAc₂ (4512-3) (downexpressed in RLS), HexNAc₆Hex₇NeuAc₃ (6703-1) (downexpressed in RLS), HexNAc₆Hex₇NeuAc₃ (6703-2) (upexpressed in RLS), and HexNAc₅Hex₆NeuAc₃ (5603-5) (upexpressed in RLS).

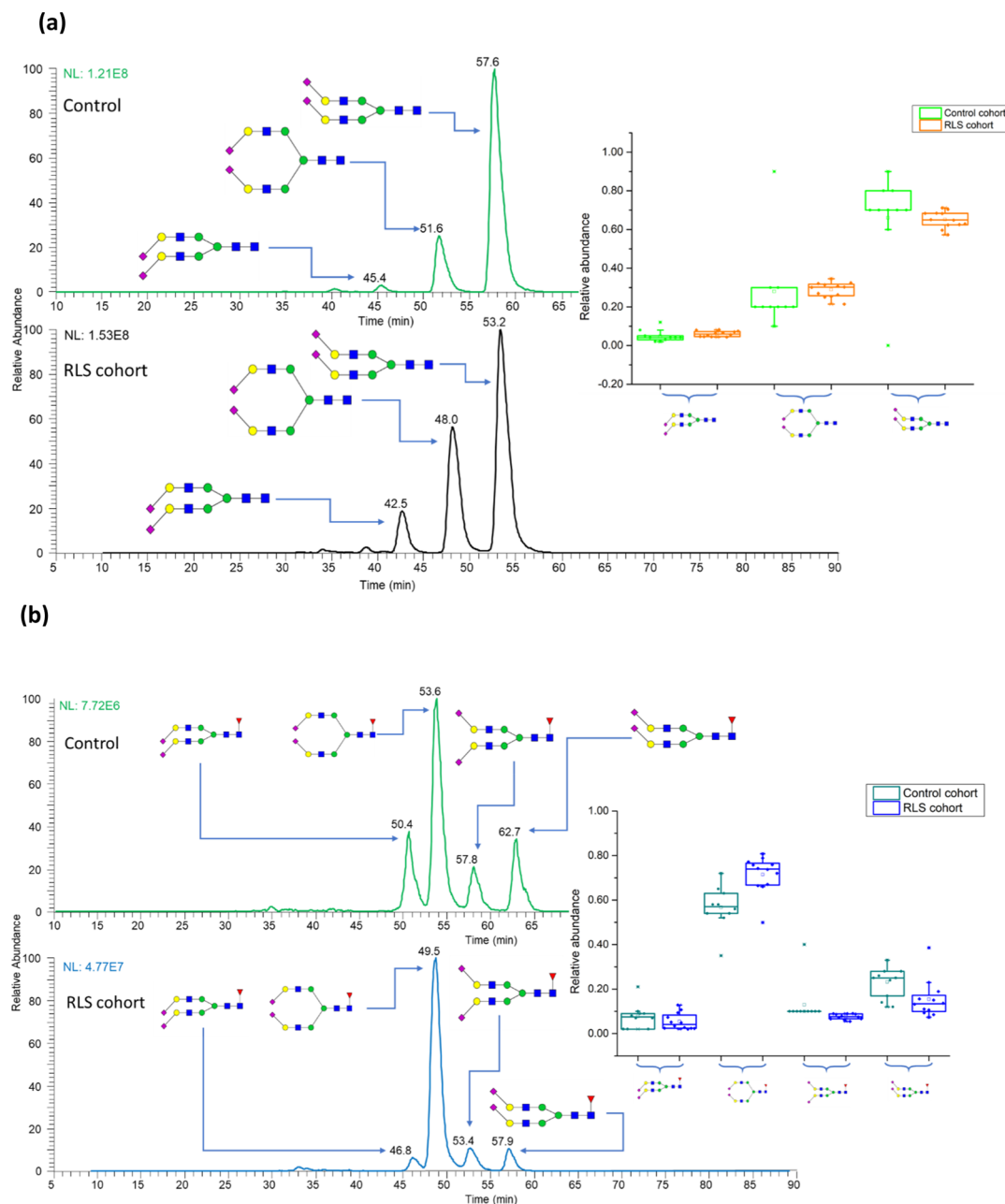


Figure 5. EICs of *N*-glycan isomers with different linkages in control and RLS cohorts, separated on PGC (a) disialylated linkage isomers (b) disialylated linkage isomers with core fucose connections. Insets are the box plots showing the distributions of disialylated isomers among 10 studied subjects in the control and 12 subjects in the RLS cohorts. The box stands for the first quartile and third quartile; the line represents median; and the whiskers above and below the box set the limits for outliers. Symbols: see Figure 2.

Although HexNAc₆Hex₇NeuAc₃ (6703-2) and HexNAc₅Hex₆NeuAc₃ (5603-5) were overexpressed in RLS, they are low in concentration in blood serum (<5%). Glycans with the composition of HexNAc₄Hex₅Fuc₁NeuAc₁ (12% in blood) and the isomeric structure HexNAc₄Hex₅Fuc₁NeuAc₁ (4511-4) (downexpressed in RLS) may be better biomarker candidates.

Isomeric analysis results (Tables S4 and S5) were also analyzed with PCA, as shown in Figure 4b. Data points of the control cohort and the RLS cohort clustered in separate areas of the PCA plot, which match the results from the glycan profile PCA. The clustering and separation in PCA indicate that the difference in the isomeric distribution of different sample points has some similarities within the same cohort and

the observed differences between the cohorts possibly represent differences related to the disease state.

Example EICs of glycan isomers with α 2-3 and α 2-6 linked sialic acids are shown in Figure 5a,b. The identifications of isomers were based on the eluting order of α 2-3- and α 2-6-linked sialic acid moieties, which were well documented in our previous studies on glycans released from model glycoproteins.^{26,27} The peaks in both figures are baseline separated and with good peak shapes that guarantee the accurate quantitation of the isomers. Figure 5a,b was only extracted from one sample in the control and RLS cohorts, respectively. In Figure 5a,b, the peak heights of isomeric peaks in the control individual and the RLS individual are different. Although the distributions of isomers among individuals are different, they cannot represent

the traits of the cohorts. The box plots (insets in both Figure 5a,b) display the distributions of all the sample points in both cohorts (10 individual samples in the control and 12 patients in the RLS cohorts, respectively) in order to show a bigger picture of how the individual data distributed in the control and RLS cohorts.

Sialic acid linkage isomers are important features to investigate in brain glycosylation studies. Studies have shown that an increase of α 2-6 linked sialic acids is usually observed in brain diseases related to viral or bacterial pathogen binding.³⁴ Changes in α 2-3 and α 2-6 linked sialic acid expressions were found in RBD,¹¹ neurodegenerative diseases,¹³ and other diseases such as cancers.¹⁷ In the brain, glycans play significant roles in signal transduction between cells. The diversity of glycans and fine specificities introduced by linkage isomers enable the tuning of different biofunctions and complex processes in the brain.³⁵ The expression levels of different glycan isomers are controlled by different glycosyltransferases. However, so far, our knowledge about the biofunctions of glycan isomers is very limited. The specific molecular mechanisms of the glycan isomers in RLS or other neurological disorders are still unknown.

CONCLUSIONS

In this study, we investigated the possible significantly altered glycan expressions in idiopathic RLS cases by comparing their serum glycan profile with that of healthy subjects. 24 *N*-glycan biomarker candidates were identified. Among those, HexNAc₆Hex₈Fuc₁NeuAc₂, HexNAc₆Hex₆Fuc₁NeuAc₃, and HexNAc₅Hex₆Fuc₁NeuAc₂ are the most significantly different structures in the expression profiles ($p < 0.001$).

Furthermore, in-depth comparative glycomics analyses were conducted by investigating the isomeric distribution in the RLS cases versus controls. Twenty-three isomeric structures showed a significant difference between the control and RLS cohorts after the Benjamini–Hochberg multiple testing correction. Among the isomers, HexNAc₄Hex₅Fuc₁NeuAc₂ (4512-3) (downexpressed in RLS), HexNAc₆Hex₇NeuAc₃ (6703-1) (downexpressed in RLS), HexNAc₆Hex₇NeuAc₃ (6703-2) (upexpressed in RLS), and HexNAc₅Hex₆NeuAc₃ (5603-5) (upexpressed in RLS) show the most significant differences. Nevertheless, the glycan with the composition of HexNAc₄Hex₅Fuc₁NeuAc₁ and the isomeric structure HexNAc₄Hex₃Fuc₁NeuAc₁ (4511-4) (downexpressed in RLS) can be better biomarker options, owing to their relatively higher abundance in blood.

The next step in analysis will be extended to a larger number of samples and a broader range of diseased and healthy cases for verification of the glycan biomarkers. The biomarker candidate's specificity and sensitivity will be assessed as well.³⁶ Herein, we just listed the changes in glycans expressed in the RLS versus the control group that can be potential glycan biomarker candidates. We hope this work will inspire other researchers to further study these glycans, especially the glycan isomers, and understand more about their biofunctions in neurological disorders and diseases.

ASSOCIATED CONTENT

Supporting Information

The Supporting Information is available free of charge at <https://pubs.acs.org/doi/10.1021/acs.jproteome.9b00549>.

Bar graphs showing the *N*-glycan isomeric distribution with a significant difference in control cohort versus RLS cohort after applying the Benjamini–Hochberg multiple testing correction; relative abundances of *N*-glycans derived from human blood sera in the control cohort; results were acquired in the C18 column at 55 °C; relative abundances of *N*-glycans derived from human blood sera in the RLS cohort; results were acquired in the C18 column at 55 °C; average relative abundances of *N*-glycans with a significant difference in control cohort versus RLS cohort after applying the Benjamini–Hochberg multiple testing correction; isomeric quantitation results in the control cohort; isomeric quantitation results in the RLS cohort; and average relative abundances of *N*-glycan isomers with a significant difference in control cohort versus RLS cohort after applying the Benjamini–Hochberg multiple testing correction (PDF)

AUTHOR INFORMATION

Corresponding Author

Yehia Mechref – Department of Chemistry and Biochemistry, Texas Tech University, Lubbock, Texas 79409-1061, United States; orcid.org/0000-0002-6661-6073; Phone: 806-834-8346; Email: yehia.mechref@ttu.edu; Fax: 806-742-1289

Authors

Xue Dong – Department of Chemistry and Biochemistry, Texas Tech University, Lubbock, Texas 79409-1061, United States

Stefania Mondello – Department of Biomedical and Dental Sciences and Morphofunctional Imaging, University of Messina, Messina 98122, Italy; Sleep Research Centre, Department of Neurology IC, Oasi Research Institute—IRCCS, Troina 94018, Italy

Firas Kobeissy – Department of Biochemistry & Molecular Genetics, American University of Beirut, Beirut 1107 2020, Lebanon; orcid.org/0000-0002-5008-6944

Raffaele Ferri – Sleep Research Centre, Department of Neurology IC, Oasi Research Institute—IRCCS, Troina 94018, Italy

Complete contact information is available at: <https://pubs.acs.org/doi/10.1021/acs.jproteome.9b00549>

Author Contributions

[†]X.D. and S.M. contributed equally to this work.

Notes

The authors declare no competing financial interest.

ACKNOWLEDGMENTS

This work was supported by NIH (1R01GM112490-04) and the Italian Ministry of Health (RC no. 2634472 and GR-2013-02354960).

REFERENCES

- (1) Merlino, G.; Valente, M.; Serafini, A.; Gigli, G. L. Restless legs syndrome: diagnosis, epidemiology, classification and consequences. *Neurol. Sci.* **2007**, *28*, S37–S46.
- (2) Catoire, H.; Sarayloo, F.; Mourabit Amari, K.; Apuzzo, S.; Grant, A.; Rochefort, D.; Xiong, L.; Montplaisir, J.; Earley, C. J.; Turecki, G.; Dion, P. A.; Rouleau, G. A. A direct interaction between two Restless Legs Syndrome predisposing genes: MEIS1 and SKOR1. *Sci. Rep.* **2018**, *8*, 12173.

- (3) Sampognaro, P. J.; Salas, R. E.; Kalloo, A.; Gamaldo, C. Restless Legs Syndrome: The Devil Is in the Details. In *Sleepy or Sleepless: Clinical Approach to the Sleep Patient*; Malhotra, R. K., Ed.; Springer International Publishing: Cham, 2015; pp 151–165.
- (4) Patton, S. M.; Cho, Y.; Clardy, T. W.; Allen, R. P.; Earley, C. J.; Connor, J. R. Proteomic analysis of the cerebrospinal fluid of patients with restless legs syndrome/Willis-Ekbom disease. *Fluids Barriers CNS* **2013**, *10*, 20.
- (5) Bellei, E.; Monari, E.; Ozben, S.; Koseoglu Bitnel, M.; Topaloglu Tuac, S.; Tomasi, A.; Bergamini, S. Discovery of restless legs syndrome plasmatic biomarkers by proteomic analysis. *Brain Behav.* **2018**, *8*, No. e01062.
- (6) Gottlieb, D. J.; Somers, V. K.; Punjabi, N. M.; Winkelman, J. W. Restless legs syndrome and cardiovascular disease: a research road map. *Sleep Med.* **2017**, *31*, 10–17.
- (7) Allen, R. P.; Picchietti, D. L.; Garcia-Borreguero, D.; Ondo, W. G.; Walters, A. S.; Winkelman, J. W.; Zucconi, M.; Ferri, R.; Trenkwalder, C.; Lee, H. B. Restless legs syndrome/Willis-Ekbom disease diagnostic criteria: updated International Restless Legs Syndrome Study Group (IRLSSG) consensus criteria - history, rationale, description, and significance. *Sleep Med.* **2014**, *15*, 860–873.
- (8) Buchfuhrer, M. J. Establishing a Diagnosis of Restless Legs Syndrome. *Clinician's Manual on Restless Legs Syndrome*; Springer International Publishing: Cham, 2016; pp 13–21.
- (9) Mondello, S.; Muller, U.; Jeromin, A.; Streeter, J.; Hayes, R. L.; Wang, K. K. Blood-based diagnostics of traumatic brain injuries. *Expert Rev. Mol. Diagn.* **2011**, *11*, 65–78.
- (10) Mondello, S.; Kobeissy, F.; Mechref, Y.; Zhao, J.; Talih, F. R.; Cosentino, F.; Antelmi, E.; Moresco, M.; Plazzi, G.; Ferri, R. Novel biomarker signatures for idiopathic REM sleep behavior disorder: A proteomic and system biology approach. *Neurology* **2018**, *91*, e1710–e1715.
- (11) Dong, X.; Mondello, S.; Kobeissy, F.; Talih, F.; Ferri, R.; Mechref, Y. LC-MS/MS glycomics of idiopathic rapid eye movement sleep behavior disorder. *Electrophoresis* **2018**, *39*, 3096–3103.
- (12) Zhu, R.; Song, E.; Hussein, A.; Kobeissy, F. H.; Mechref, Y. Glycoproteins Enrichment and LC-MS/MS Glycoproteomics in Central Nervous System Applications. *Methods Mol. Biol.* **2017**, *1598*, 213–227.
- (13) Abou-Abbass, H.; Abou-El-Hassan, H.; Bahmad, H.; Zibara, K.; Zebian, A.; Youssef, R.; Ismail, J.; Zhu, R.; Zhou, S.; Dong, X.; Nasser, M.; Bahmad, M.; Darwish, H.; Mechref, Y.; Kobeissy, F. Glycosylation and other PTMs alterations in neurodegenerative diseases: Current status and future role in neurotrauma. *Electrophoresis* **2016**, *37*, 1549–1561.
- (14) Abou-Abbass, H.; Bahmad, H.; Abou-El-Hassan, H.; Zhu, R.; Zhou, S.; Dong, X.; Hamade, E.; Mallah, K.; Zebian, A.; Ramadan, N.; Mondello, S.; Fares, J.; Comair, Y.; Atweh, S.; Darwish, H.; Zibara, K.; Mechref, Y.; Kobeissy, F. Deciphering glycomics and neuroproteomic alterations in experimental traumatic brain injury: Comparative analysis of aspirin and clopidogrel treatment. *Electrophoresis* **2016**, *37*, 1562–1576.
- (15) Varki, A. Biological roles of glycans. *Glycobiology* **2017**, *27*, 3–49.
- (16) Veillon, L.; Fakhri, C.; Abou-El-Hassan, H.; Kobeissy, F.; Mechref, Y. Glycosylation Changes in Brain Cancer. *ACS Chem. Neurosci.* **2018**, *9*, 51–72.
- (17) Peng, W.; Zhao, J.; Dong, X.; Banazadeh, A.; Huang, Y.; Hussien, A.; Mechref, Y. Clinical application of quantitative glycomics. *Expert Rev. Proteomics* **2018**, *15*, 1007–1031.
- (18) Zhou, S.; Veillon, L.; Dong, X.; Huang, Y.; Mechref, Y. Direct comparison of derivatization strategies for LC-MS/MS analysis of N-glycans. *Analyst* **2017**, *142*, 4446–4455.
- (19) Kailemia, M. J.; Ruhaak, L. R.; Lebrilla, C. B.; Amster, I. J. Oligosaccharide analysis by mass spectrometry: a review of recent developments. *Anal. Chem.* **2013**, *86*, 196–212.
- (20) Dong, X.; Huang, Y.; Cho, B. G.; Zhong, J.; Gautam, S.; Peng, W.; Williamson, S. D.; Banazadeh, A.; Torres-Ulloa, K. Y.; Mechref, Y. Advances in mass spectrometry-based glycomics. *Electrophoresis* **2018**, *39*, 3063–3081.
- (21) Hu, Y.; Mechref, Y. Comparing MALDI-MS, RP-LC-MALDI-MS and RP-LC-ESI-MS glycomic profiles of permethylated N-glycans derived from model glycoproteins and human blood serum. *Electrophoresis* **2012**, *33*, 1768–1777.
- (22) Dong, X.; Zhou, S.; Mechref, Y. LC-MS/MS analysis of permethylated free oligosaccharides and N-glycans derived from human, bovine, and goat milk samples. *Electrophoresis* **2016**, *37*, 1532–1548.
- (23) Mechref, Y.; Kang, P.; Novotny, M. V. Solid-phase permethylation for glycomic analysis. *Methods Mol. Biol.* **2009**, *534*, 53–64.
- (24) Hu, Y.; Desantos-Garcia, J. L.; Mechref, Y. Comparative glycomic profiling of isotopically permethylated N-glycans by liquid chromatography/electrospray ionization mass spectrometry. *Rapid Commun. Mass Spectrom.* **2013**, *27*, 865–877.
- (25) Zhou, S.; Hu, Y.; Mechref, Y. High-temperature LC-MS/MS of permethylated glycans derived from glycoproteins. *Electrophoresis* **2016**, *37*, 1506–1513.
- (26) Zhou, S.; Dong, X.; Veillon, L.; Huang, Y.; Mechref, Y. LC-MS/MS analysis of permethylated N-glycans facilitating isomeric characterization. *Anal. Bioanal. Chem.* **2017**, *409*, 453–466.
- (27) Zhou, S.; Huang, Y.; Dong, X.; Peng, W.; Veillon, L.; Kitagawa, D. A. S.; Aquino, A. J. A.; Mechref, Y. Isomeric Separation of Permethylated Glycans by Porous Graphitic Carbon (PGC)-LC-MS/MS at High Temperatures. *Anal. Chem.* **2017**, *89*, 6590–6597.
- (28) Hu, Y.; Zhou, S.; Yu, C.-Y.; Tang, H.; Mechref, Y. Automated annotation and quantitation of glycans by liquid chromatography/electrospray ionization mass spectrometric analysis using the MultiGlycan-ESI computational tool. *Rapid Commun. Mass Spectrom.* **2015**, *29*, 135–142.
- (29) Yu, C.-Y.; Mayampurath, A.; Hu, Y.; Zhou, S.; Mechref, Y.; Tang, H. Automated annotation and quantification of glycans using liquid chromatography-mass spectrometry. *Bioinformatics* **2013**, *29*, 1706–1707.
- (30) Huang, Y.; Zhou, S.; Zhu, J.; Lubman, D. M.; Mechref, Y. LC-MS/MS isomeric profiling of permethylated N-glycans derived from serum haptoglobin of hepatocellular carcinoma (HCC) and cirrhotic patients. *Electrophoresis* **2017**, *38*, 2160–2167.
- (31) Cho, B. G.; Veillon, L.; Mechref, Y. N-Glycan Profile of Cerebrospinal Fluids from Alzheimer's Disease Patients Using Liquid Chromatography with Mass Spectrometry. *J. Proteome Res.* **2019**, *18*, 3770–3779.
- (32) Peng, W.; Goli, M.; Mirzaei, P.; Mechref, Y. Revealing the Biological Attributes of N-Glycan Isomers in Breast Cancer Brain Metastasis Using Porous Graphitic Carbon (PGC) Liquid Chromatography-Tandem Mass Spectrometry (LC-MS/MS). *J. Proteome Res.* **2019**, *18*, 3731–3740.
- (33) Fogli, A.; Merle, C.; Roussel, V.; Schiffmann, R.; Ughetto, S.; Theisen, M.; Boespflug-Tanguy, O. CSF N-Glycan Profiles to Investigate Biomarkers in Brain Developmental Disorders: Application to Leukodystrophies Related to eIF2B Mutations. *PLoS One* **2012**, *7*, No. e42688.
- (34) Varki, N. M.; Varki, A. Diversity in cell surface sialic acid presentations: implications for biology and disease. *Lab. Invest.* **2007**, *87*, 851–857.
- (35) Schnaar, R. L.; Gerardy-Schahn, R.; Hildebrandt, H. Sialic acids in the brain: gangliosides and polysialic acid in nervous system development, stability, disease, and regeneration. *Physiol. Rev.* **2014**, *94*, 461–518.
- (36) Rifai, N.; Gillette, M. A.; Carr, S. A. Protein biomarker discovery and validation: the long and uncertain path to clinical utility. *Nat. Biotechnol.* **2006**, *24*, 971–983.